

Article

# Biomechanical Performance of the Cemented Hip Stem with Different Surface Finish

Jui-Pin Hung <sup>1,\*</sup> , Yu-Wei Bai <sup>2</sup>, Chung-Qua Hung <sup>1</sup> and Tsui-Er Lee <sup>3</sup>

<sup>1</sup> Graduate Institute of Precision Manufacturing, National Chin-Yi University of Technology, Taichung 41170, Taiwan; narusawa30@gmail.com

<sup>2</sup> Department of Mechanical Engineering, National Chin-Yi University of Technology, Taichung 41170, Taiwan; feast5158@gmail.com

<sup>3</sup> Office of Physical Education, Asia University, Taichung 41354, Taiwan; vivian@asia.edu.tw

\* Correspondence: hungjp@ncut.edu.tw; Tel.: +886-4-2392-4505 (ext. 7181); Fax: 886-4-2392-5714

Received: 10 August 2019; Accepted: 26 September 2019; Published: 30 September 2019



**Abstract:** The integrity of the cemented fixation interface is responsible for the long-term longevity of artificial hip prostheses. Metallic stems with roughened surfaces are considered to provide stronger adhesion with cement. However, clinical studies have reported that roughened stems show a lower survival rate than polished stems. These studies clearly reveal that the causes of artificial stem loosening are very complicated and multifaceted. Therefore, this study was conducted to investigate the mechanical effect of stem surface finish in cemented hip replacement. To accomplish this, a series of cement–metal specimens were tested configurations to assess the mechanical characteristics of the cement–metal interface specimens. A finite elemental model of cemented femoral prostheses was then created, in which the cement–stem interface was assumed to be in different bonding states according to the experimentally measured interface properties. The failure probabilities of the cement mantle and cemented interface under physiological loadings were evaluated. Experimental results indicate that the polished metal produced higher interfacial tensile and lower shearing strengths than the roughened metal. The polished stems were predicted to induce a lower failure probability of cement mantle and higher integrity of the cement–stem interface when compared to the roughened stem. Overall, current results provide significant evidence to support the clinical outcomes of cemented hip prostheses with different stem surface finishes.

**Keywords:** aseptic loosening; cemented implant; interfacial strength; surface finish

## 1. Introduction

Artificial stems implanted in bone marrow cavities with bone cement have become the major method of surgical fixation, since this method can provide initial or immediate stability to the prosthetic component. However, from clinical observations, it was found that, in some cases of artificial hip prostheses, revision is required owing to loosening of the cemented component after long-term use. Numerous studies have shown that the causes of artificial stem loosening are very complicated and multifaceted [1–5]. The main causes of early loosening of artificial prostheses are deterioration of the bonded interface between the metal stem and the cement mantle and between the bone and the cement mantle [4,5].

It is well known that implant loosening can originate from cement–stem interfaces, especially around the proximal and distal regions of femur bone. Interface failure can be caused by the higher mechanical stress induced at the cemented interfaces under gait loading. Hence, the bonding strength and stress level of the cement–stem interface are crucial factors that determine the success or failure of the fixation of total joint replacements. Conversely, even when the interfacial bonding strengths

have been shown to improve in response to the surface finish of metallic stems under experimental configurations, the clinical effects of stem surface treatments in orthopedic applications have been controversial with regard to mechanical failure of femoral prostheses.

Various treatments of the outer surface of the metal prosthetic stem, including surface polishing, proximal porous coatings, and roughening of textures by grit-blasting, have been employed to enhance the ability of these prostheses to bond with cement [6–8]. Interfacial strengths have been characterized in the tensile or shearing loading modes under different testing configurations [9–13]. For example, the push-off or pull-out testing configuration has been used to measure the shear strength of the interface. These methods have enabled the identification of potential factors influencing bonding strength. The interfacial shear strength has been shown to increase with increasing surface roughness of the metal stem [12,13]. However, the relationship between tensile bonding strength and surface morphology cannot be confirmed owing to the inconsistent results obtained from different experiments [12–14].

On the other respect, total hip replacement (THR) using either smooth or rough femoral stems has resulted in good performance, as assessed during intermediate postoperative periods [15–17]. However, the roughened stems were found to induce higher debonding rates at the cement–prosthesis interface [2,18,19]. Comparative studies have also reported that roughened prostheses were more susceptible to aseptic loosening than polished stems [20]. Contrarily, primary THR with a cemented polished stem was verified to show excellent results in young patients [21]. Clinical studies relating to cemented implants reported polished tapered stems had a significantly lower revision rate of femoral revision when compared with matt surface stems [22]. Although the causes of the loosening after implantations vary considerably, the continuous fretting wear at the stem–bone–cement interface has been regarded as a type of wearing mechanism causing the failure of the arthroplasty with both matt and polished cemented stems [23]. The influence of surface processing on the tribocorrosion at the cemented interface have been reported in studies [9,24,25], for example, Bryant et al. [24] reported that fretting corrosion of metal stems has been implicated in the early failure and high revision rates of the polished femoral stems. They also demonstrated that a polished surface might cause higher levels of tribocorrosion and ion release when compared to the blasted surfaces. Investigations of retrieved cemented femoral implants showed that wear induced tribocorrosive interaction at the bonding interface would damage the surface of the polished CoCr femoral stems [25].

Concluding from abovementioned literature, we believe that the mechanical effect associated with the use of surface-treated stems in cemented hip replacement warrants further investigation and clarification. In the present study, we investigated the mechanical effect of stem surface finishes by mechanical strength tests and the finite element modeling approach. To accomplish this, a series of cement–metal specimens were used to assess the interfacial strengths under different loading modes. Correlations between the metal surface morphology and interface strength were also established. Two finite element models of the cemented femoral composite structure with roughened and polished stems were then created. Some assumptions were made in modeling of the cemented prostheses, as follows: the interfaces between cement and metal stem were assumed to be evenly bonded with elastic layers with homogenous mechanical properties. Also, the interfacial strengths at the cement–stem interfaces were consistent respectively throughout the entire bonding surfaces. The failure probabilities of the cement mantle and cemented interface for the two models were evaluated and compared to assess the effects of the stem surface finish. The results obtained from the finite element modeling were employed to clarify the mechanical failure phenomena observed in total hip replacements.

## 2. Experimental Work

### 2.1. Specimen Preparation and Mechanical Tests

To assess the bonding strength of the interface between bone cement and the metal stem, a number of specimens were prepared from acrylic bone cement and metal samples. The configuration and dimension of the cement–metal specimens are depicted in Figure 1. Preparation procedures for these

interfacial specimens are briefly described as follows. First, metal samples of medium carbon steel were machined into rectangular shapes ( $30 \times 10 \times 5$  mm). To investigate the influence of surface roughness on the interfacial bonding strength, these samples were then divided into two groups—those with a smooth surface and those with a rough surface (Figure 2). The bonding surface of each metal sample was then fine-machined to be smooth ( $R_a = 0.14 \mu\text{m}$ ), while samples in the rough surface group were sand-blasted to a roughness of  $5.56 \mu\text{m}$  approximately. The bone cement was then prepared by mixing PMMA (Polymethyl methacrylate) polymer powder with a liquid monomer in a container according to the manufacturer's guidelines. The metal samples were individually placed in mold cavities, after which mixed bone cement was added. Manually exerted pressure was maintained during curing to ensure firm bonding with the metal samples. After the bone cement polymerized, the specimens were carefully removed from the mold cavities and verified by visual examination to ensure their integrity for testing.

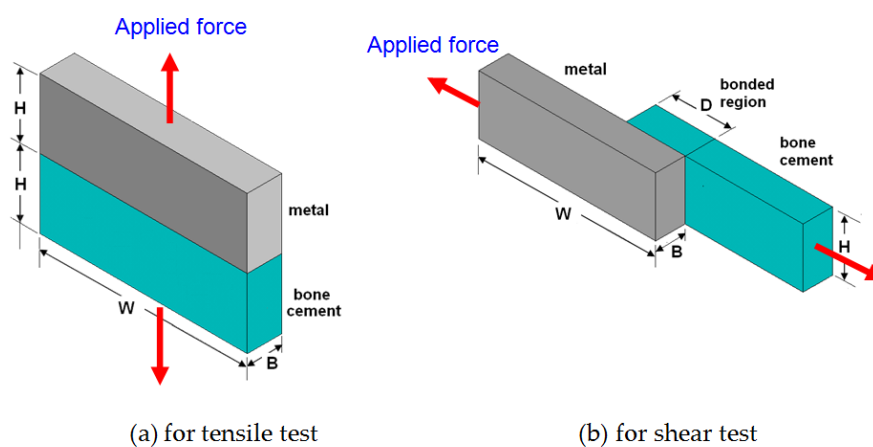


**Figure 1.** Geometry dimensions of metal/cement specimens and testing configuration for tensile and shear tests, respectively. ( $W = 30$  mm,  $H = 10$  mm,  $B = 5$  mm,  $D = 10$  mm).

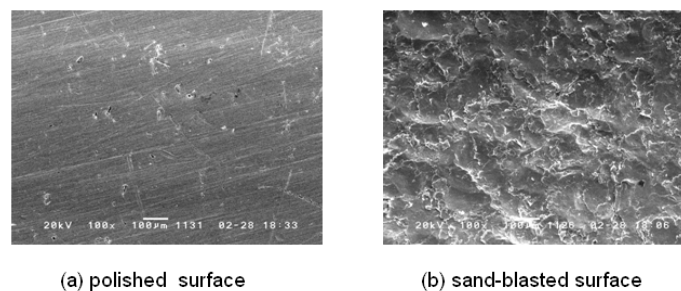


**Figure 2.** Surface topography of the metal specimens (a) polished; (b) sand-blasted.

The specimens were separately fixed in custom grips for tests using a computerized universal testing machine (Figure 1). During testing, the upper crosshead imposed a tensile force on the specimen at a rate of  $2.0$  mm/min until the interface failed completely. The critical load  $F_{cr}$  at the fracture instant was obtained from the load–displacement diagram recorded by the computerized data acquisition system. This information was then used to calculate the interfacial strength according to the formula  $F_{cr}/A$ , where  $A$  is the bonding area between the metal and bone cement. Additionally, the load–displacement diagram was converted into a stress–displacement curve by dividing the applied force by the bonding area, as illustrated in Figure 3. The slope of the stress–displacement curve represented the relative stiffness  $K_{int}$  of the interface between the bone cement and the metal. This curve was determined by applying the least squares fitting procedure to the stress–displacement curve for applied stress levels of less than 50% of the failure strength [20].

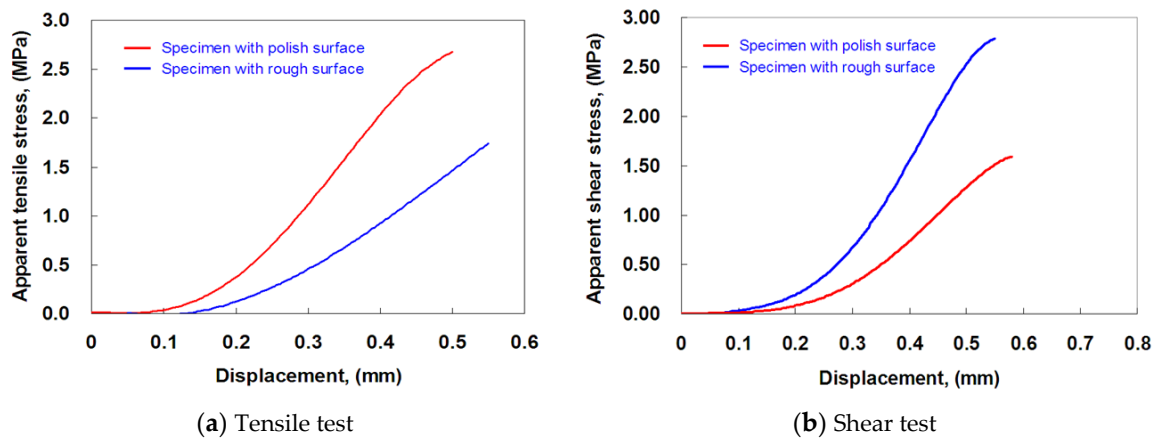


**Figure 3.** Typical relationship between the surface traction and displacement of the bonded interface under tensile and shear loading, respectively.

### 2.2. Interface Strengths

The bonding strengths of the cement–metal specimens obtained from the mechanical tests are presented as the mean value  $\pm$  the standard deviation and are summarized in Table 1. The tensile and shear strengths of the interface between the cement and the roughened metal specimen were 1.73 ( $\pm 0.61$ ) MPa and 3.80 ( $\pm 0.48$ ) MPa, respectively. For specimens bonded with cement and polished metal specimens, the tensile strength was measured as 2.81 ( $\pm 1.15$ ) MPa and the shear strength as 1.39 ( $\pm 0.55$ ) MPa. The normal and tangential stiffness of the interface formed with the sand-blasted surfaces were 15.48 ( $\pm 5.05$ ) MPa/mm and 13.95 ( $\pm 3.807$ ) MPa/mm, respectively. However, for polished surfaces, the normal and tangential stiffness of the interface were 19.17 ( $\pm 8.62$ ) MPa/mm and 8.21 ( $\pm 2.28$ ) MPa/mm, respectively.

**Table 1.** Interface tensile strength and bonding stiffness for cement/metal specimens.

Surface Roughness of Metal Specimen	Under Tensile Loading		Under Shearing Loading	
	Strength (MPa)	Stiffness (MPa/mm)	Strength (MPa)	Stiffness (MPa/mm)
Polished surface Ra = 0.6 $\mu\text{m}$	2.81 $\pm$ 1.15 (n = 22) *	19.17 $\pm$ 8.62 (n = 22) *	1.39 $\pm$ 0.55 (n = 15) *	8.71 $\pm$ 3.91 (n = 15) *
Sand-blasted surface Ra = 6 $\mu\text{m}$	1.73 $\pm$ 0.61 (n = 18) *	15.48 $\pm$ 5.05 (n = 18) *	3.80 $\pm$ 0.48 (n = 18) *	13.95 $\pm$ 3.81 (n = 18) *

\* Value (n) represents the number of specimens for tests.

One-way ANOVA indicates that there is a significant difference between the interfacial strengths generated by metals with smooth surfaces and with rough surfaces, with a *p*-value of 0.009 for both tensile and shearing strengths. Compared to roughened surfaces, polished surfaces showed superior bonding strength and normal stiffness in resisting interface separation under tensile loading (*p* = 0.009). Conversely, the roughened metals showed higher interfacial shear strength and tangential stiffness than the polished metal in resisting shearing deformation.

Several experimental studies with various configurations of the specimen showed different results [9–13,26–28], which makes direct comparisons of interfacial bonding strength among studies difficult. For example, Davies and Harries [9] reported that the tensile bonding strength between grit-blasted CoCr rods (Ra = 1–2  $\mu\text{m}$ ) and bone cement was about 5.0 MPa. In contrast to the positive tendency in the variation of tensile strength observed with surface roughness, Pittman et al. [10] reported that polished metal rods had an inferior tensile bonding strength with cement when compared to roughened metal rods. They found that the tensile strength of the bonded interface was about

7.3–9.9 MPa for metallic rods with coarse grit-blasted surfaces ( $R_a = 6.67 \mu\text{m}$ ), but was 2.7–4.9 MPa for metal samples with a blasted ceramic coating ( $R_a = 0.97 \mu\text{m}$ ). Keller et al. [26] conducted pull-off tests of cement–metal bonded specimens and found that polished metal ( $R_a = 0.1 \mu\text{m}$ ) yielded higher tensile bonding strength than roughened metal ( $R_a = 15 \mu\text{m}$ ).

In a study conducted to investigate interfacial shear strength, Chen et al. [7] showed that the shear strength of the cement–metal interface ranged from 0.56 to 1.89 MPa, and that the values were positively related to the surface roughness of the metal specimen. Wang et al. [16] also reported that the interfacial shear strengths were 0.53 and 9.85 MPa for polished ( $R_a = 0.03 \mu\text{m}$ ) and grit-blasted ( $R_a = 4.65 \mu\text{m}$ ) surfaces. Recent investigations by Zhang et al. [11,13] showed that steel rods with polished or blasted surface roughness exhibited different shearing strengths: 2.95 MPa in the case of polished rods ( $R_a = 0.56 \mu\text{m}$ ), 4.36 MPa for glass bead-blasted rods ( $R_a = 1.33 \mu\text{m}$ ), and 16.42 MPa for grit-blasted rods ( $R_a = 5.21 \mu\text{m}$ ). Zelle et al. [14] found that the mixed-mode interface strengths of the cement–implant specimens were positively related to the surface roughness generated by a grit-blasting method. For varying surface roughness ( $R_a = 0.89\text{--}2.76 \mu\text{m}$ ), the interface strengths under pure shear and tensile loadings were measured as 1.95–9.90 MPa and 0.58–6.67 MPa, respectively.

Overall, these findings indicate that tensile and shear bonding strengths vary greatly, and that there is considerable discrepancy among measurements. A well-known phenomena that has been revealed in the present study and previous studies [7,12,13] is that metal samples treated by the sand-blasting method showed superior bonding ability with cement against shearing force when compared to smooth metals. Meanwhile, we found that the polished surface produced a higher interfacial bonding strength than the sand-blasted surface when resisting tensile loading. In addition, reviewing the published works [11,13,14], we can find that a variety of cement of different type and viscosity were used for the preparation of stem–cement interface specimens, which also contributed to a great variation in the measured interface strengths, apart from the variability induced by metal samples with different surface morphology.

According to studies [12], a bonding surface with higher roughness may allow more cement to flow into the cavities between surface asperities, thereby generating a better bonding layer to resist shear force. A less roughened surface processed by bead or grit-blasted method would produce a lower bonding strength under shearing and tensile loading because of weaker adhesion with the cement [12–14,29]. However, more gaps were also found to form at the interface between the cement and the roughened stem, which indicated that the cement was not well integrated with the rougher surface [29]. This effect might bring to the measurement of Iesaka et al. [30] that the matte stem surfaces generated lower interfacial shear strength than the polished with stem preheating. Conversely, a polished surface with less surface asperities might create uniform and strong adhesive layers between the cement and metal, thereby enhancing resistance against tensile forces [26].

### 3. Modeling of the Stem Cemented in Femur

#### 3.1. Interface Model

The mechanical behavior of the bonded interface could be studied from the tensile and shear tests. As shown in Figure 3, the cement–metal interface under tensile loading exhibits a linear relationship between apparent stress and displacement after the initial loading stage. Within the linear region, the surface traction (or apparent stress)  $T_i$  can be related to the relative displacement  $\delta_i$  of the bonded surfaces by the following constitutive equation:

$$\begin{aligned} T_n &= K_{in} \cdot \delta_n & T_n &\leq \sigma_u, \\ T_s &= K_{is} \cdot \delta_s & T_s &\leq \tau_u. \end{aligned} \quad (1)$$

In the above equation,  $K_{in}$  and  $K_{is}$  are the stiffness values calibrated in the normal and tangential directions to the interface, respectively, which also represent the ability of the interface to resist the relative deformation of the bonded materials.

For development of the finite element model of a cemented stem, the spring layer model used in fracturing analysis of bimaterial adhesive joint structure [31,32] was employed to simulate the mechanical characteristics of the cement–stem interface. The interdigitated region between the bone cement and the stem was considered to be the adhesive layer, which was replaced by spring elements distributed over this layer (Figure 4). Each spring element connecting the node pairs at the cement and stem element was characterized based on the stiffness and strength along the normal or tangential directions of the interfaces, respectively.

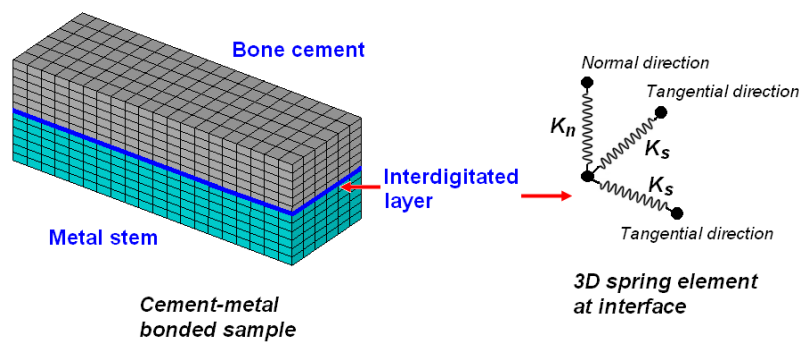


**Figure 4.** Schematic of the spring layer used to model the bonding between the bone cement and metal stem.

### 3.2. Finite Element Modeling

A finite element model of cemented hip prostheses was established to analyze the stress state under physiological gait loadings (Figure 5). The femur model consisted of the femur bone, metal stem, and the cement mantle. The metal stem had the following dimensions: distal diameter = 15 mm, stem length = 166 mm, offset = 45 mm, and neck length = 41 mm. Although the cross-section of the cement mantle varied along the stem shape from the proximal to the distal end, it had a constant thickness of 3.0 mm, which is within the ideal thickness range of 2–5 mm for clinical use [33].

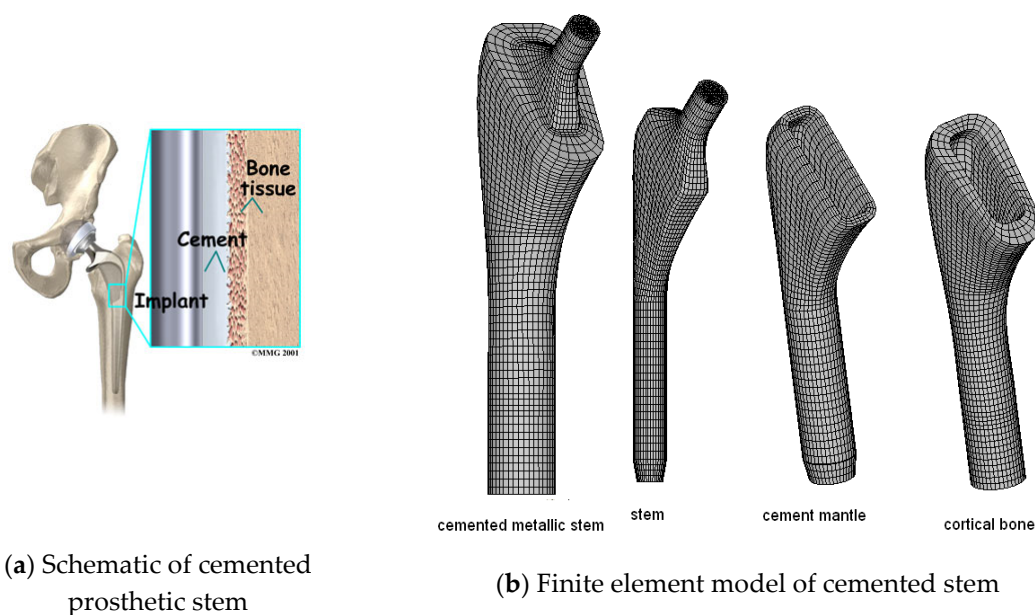


**Figure 5.** (a) schematic of cemented prosthetic stem [34]; (b) finite element model of the cemented femoral components, including stem, cement layer and femoral cortical bone.

The entire model was meshed with hexahedron brick elements, resulting in the formation of 35,520 elements and 41,914 nodes. The interfaces between the cement and bone were assumed to be

perfectly bonded, while interfaces between the metal stem and the bone cement were modeled as elastic spring layers. Using this modeling approach, the cement–stem interfaces were characterized by spring elements with adequate stiffness, which was experimentally determined from the bonding specimens. In the case of cemented model with polished stem (0.14  $\mu\text{m}$ ), the normal and tangential stiffness values of the spring elements were assumed to be 19.17 and 8.21 MPa/mm, respectively. The corresponding values assumed for the model with the sand-blasted stem (5.56  $\mu\text{m}$ ) were 15.48 and 13.95 MPa/mm, respectively. With the assumption that the bone cement and metal stem were assumed to be evenly bonded with elastic layers with homogenous interfacial stiffness, in the FE-model, the stiffness constant of each spring element is calculated from the overall stiffness divided by total spring elements on the bonding surface. The materials used for the finite element model were modeled as linear isotropic, with a Young’s modulus of 210, 15.5, and 2.28 GPa for the metallic stem, compact bone, and acrylic bone cement, respectively. Poisson’s ratio was set to 0.3 for all the materials [35].

The physiological femoral loadings applied to the cemented model were based on a previous study [36], and included the joint forces and muscle forces. The maximum joint forces were calculated as 4.6 times the body weight at 45% of the normal walking gait cycle. The muscle forces induced at this gait instant are primarily derived from the action of the abductor muscles located on the greater trochanter (gluteus medius and gluteus minimus) and ilio-tibia muscles (gluteus maximus and tensor fascia latae). These force components generated at 45% gait phase for a body weight of 70 kg were calibrated and are listed in Figure 6. All nodes at the distal end of the femur bone were constrained in all directions.

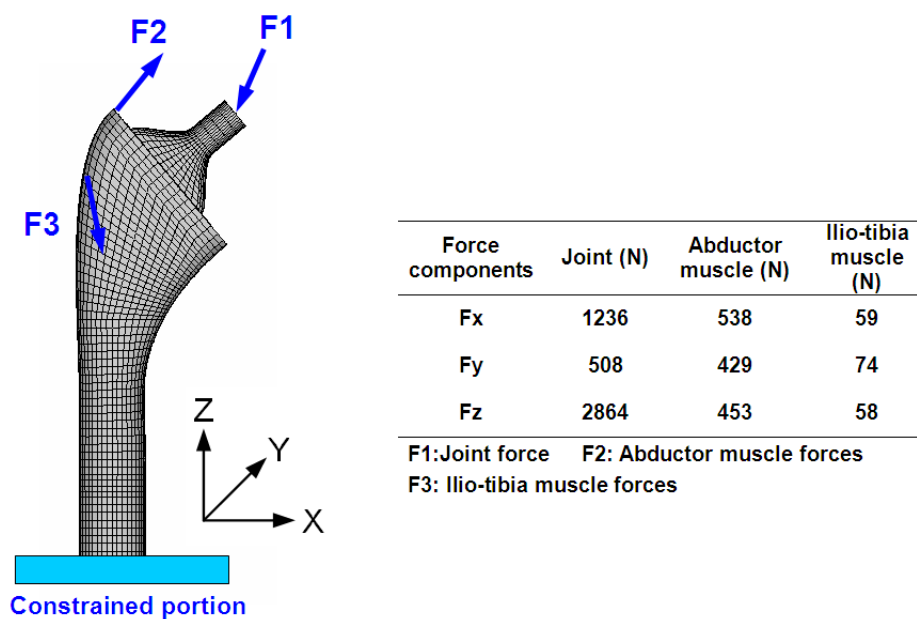


**Figure 6.** Schematic of joint force and muscle forces acting on the femoral head and femoral bone, which also shows the force components of gait loadings induced at gait phase of 45%.

#### 4. Analysis Results

##### 4.1. Overall Stress Patterns of Cemented Components

The stress states and the failure modes at the bone cement–implant interface and cement mantle were examined in this analysis since these sites were found leading to earlier failure of cemented implants. As shown in Figure 7, the maximum stress of the stem was concentrated at the central region on the medial side. The maximum stress of the femur bone was induced in the intermediate region of the posterior lateral side. For the bone cement, the regions with higher stress were primarily found at the proximal lateral portion around the stem. Apart from this region, the majority of the cement

was subjected to <6 MPa of stress. The maximum tensile stress in the proximal region was about 13 MPa, which was well below the cement tensile strength of 31–51 MPa [37], but higher than the fatigue strength of 8–10 MPa [38].

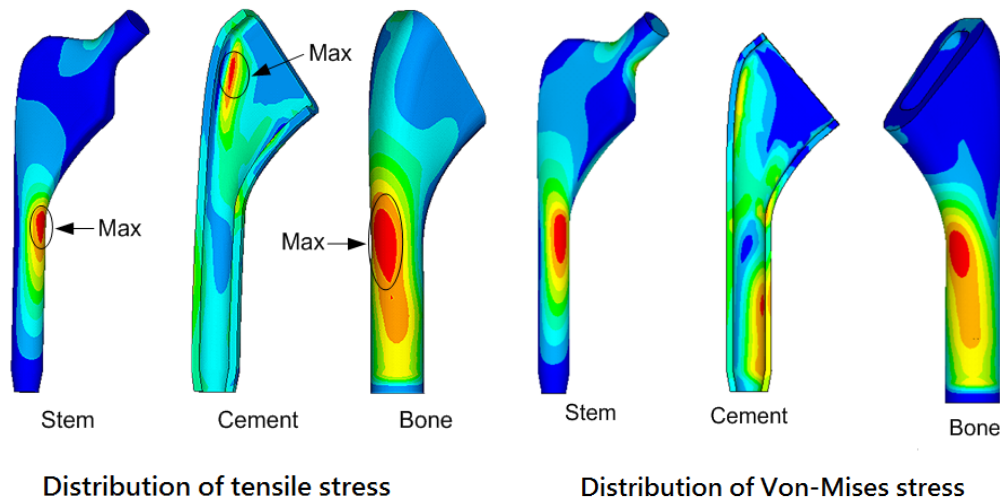


**Figure 7.** Distributions of maximum tensile stress and Von-Mises stress within stem, cement and femur bone.

#### 4.2. Probability of Failure of the Cement Mantle

Generally, the peak stress in the distal region of the cement was primarily the result of stress concentration in the distal end of the metal stem and the bending effect of joint loading [39]. To avoid inappropriate evaluation of cement stress with the use of peak tensile stress, another approach based on the stressed volumes of the cement mantle associated with the failure probability at a specific stress level was suggested to provide a better illustration of the durability of the cemented fixations [36]. The stressed volume of cement was defined by the number of elements subjected to specific stress levels. The probability of failure of the cement under specific stress levels was evaluated according to the criterion proposed in a study conducted by Murphy and Prendergast [40]. The probability of survival of cement specimens at 10 million loading cycles for hand-mixed cement can be expressed as a function of the applied stress by the following regression polynomial:

$$P_s = -0.0005\sigma^3 + 0.0202\sigma^2 - 0.3304\sigma + 1.8365. \quad (2)$$

The failure probability of the cement mantle can be determined from  $P_f = 1 - P_s$ . It should be noted that the critical stress causing the cement to endure 10 million loading cycles without failure is about 3 MPa based on Equation (2). Using this approach, the percentages of the stressed volume of the cement mantle produced by stems with different surface finishes were obtained (Figure 8). The results revealed that, for roughened and polished stems, the majority of cement mantles (about 71%) were subject to lower stress of 4 MPa. The volume fraction of cement enduring 4–8 MPa stress was about 3.5–14%. According to Equation (2), the cement mantle would be stressed to fail completely after experiencing 10 million loading cycles at 10 MPa. Therefore, as presented in Figure 8, the volume fraction of cement mantle with survival life less than 10 million stress cycles is about 1.8% for roughened stem and 1.35% for polished stem, respectively. The volume fraction of damaged cement is not be significant in value, but differed by 75%. This seems to imply that the roughened stems tended to induce a higher cement failure rate than the polished stems. It can be expected that, if the long-term loading effects with debonded interface are involved [32], the difference in damaged rate of cement mantle for polished and roughened surface stems will be more significant.

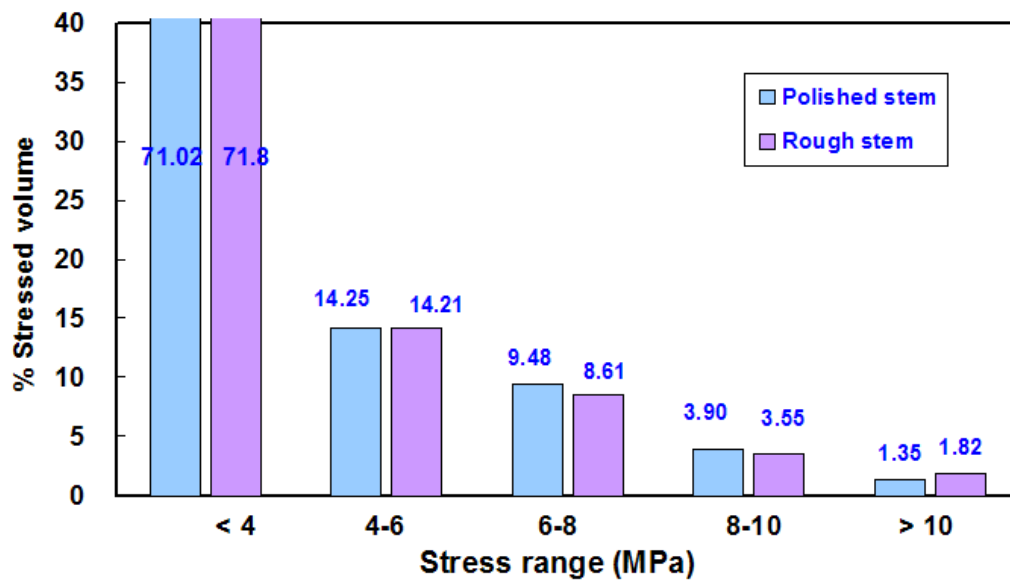


Figure 8. Comparison of the stressed volume of cement mantle at different stress range produced by the stem with smooth and rough stem.

#### 4.3. Interfacial Failure Analysis of the Cement–Stem Interface

Table 2 presents the maximum tensile and shear stress induced at cement–stem interfaces, which were found to occur near the distal end of the stems, with a localized characteristic. The maximum interfacial tensile and shear stresses generated by a smooth stem were 10.6 and 6.27 MPa, respectively. For roughened stems, the maximum tensile and shear stresses were approximately 10.52 and 7.42 MPa, respectively. Since the integrity of the bonded interface was responsible for the long-term longevity of artificial hip replacement [2,5], the extent of the failed interface was used to evaluate the performance of the cemented implants. The failure of the interface was quantified in the local region where the predicted stress exceeded the measured strength of the interface. As indicated in Table 2, for failure of the tensile mode, the percentage of interface failure induced by a roughened stem was 1.68%, while that induced by a smooth stem was about 0.96%. These findings indicated that the roughened stem tended to increase the interfacial separation rate when compared to the polished stem. Conversely, under the shearing failure mode, the percentage of failed interface around a smooth stem was 5.96%, which was higher than that around a roughened stem (3.47%). Additionally, the relative displacement of the cement–stem interface produced by polished and roughened stems was 65 and 46 μm, respectively. Compared to stems with a smooth surface, stems with a roughened surface demonstrated superior ability to resist the relative micro-motion and shear failure along the cement–stem interface. Interface failure analysis indeed give some implications to the enhancement of bonding strength and reduction of stress level for maintaining the integrity of the cement–stem interface in cemented hip prosthesis.

Table 2. Maximum stress induced within cemented femoral components under gait phase of 45%.

Surface Roughness	Maximum Interfacial Stress (MPa)		Percentage of Failed Interfaces (%)	Maximum Interface Micromotion (μm)
	At Proximal Medial Region	At Distal Lateral Region		
	Tension/Shear	Tension/Shear	Tensile/Shear Failure	
Smooth	2.11/3.92	10.62/6.20	0.90/5.96	65
Rough	1.50/4.24	10.52/7.42	1.68/3.47	46

## 5. Discussion

### 5.1. Effects of Stem Surface Finish on Interfacial Failure

The purpose of this study was to clarify the mechanical effects of the surface finish of the metal stem used in artificial hip replacement. As indicated in Table 1, the interfacial tensile and shear strengths varied with the surface finish of the metal samples, but showed an opposite tendency. Experimental results verified that the interfacial tensile strength of the polished specimen was higher than that of the roughened surface. Conversely, the sand-blasted metal showed higher bonding ability with the cement than the polished metal in resistance of shearing force.

Current experiments clearly established the correlation between the surface finish of the metal specimen and interfacial strength. However, the mechanical effect associated with the use of polished or roughened stems in femoral prosthetic replacement should be examined to clarify the controversy encountered in clinical practice. Previous studies [1,2] reported that the local fatigue damage of cement mantle and corruption of the cement/implant interface were responsible for the failure of the cemented interface in hip prosthesis. Therefore, the stresses generated in the cement mantle and at the cement–stem interface were examined to get a general view of the mechanical behavior of the hip prosthesis. However, an attempt to examine the influence of the surface finish in this manner was unsuccessful since the overall cement stress pattern generated by the polished and roughened stems was comparable. Lennon et al. [36] showed that the mechanical performance of a hip prosthesis could be quantified based on probability analysis combined with the stressed volume concept. Using this method, we identified the influence of the stem surface finish in terms of the amount of damaged cement and percentage of interface failure. As shown in Figure 8, the volumetric percentage of the damaged cement and interface failure generated by the polished stems were lower than those generated by roughened stems. These findings demonstrated that the polished stems were superior to the roughened stems with respect to enhancing the mechanical performance of cemented prostheses. These findings are comparable to those of previously conducted studies [29,30].

Many previous studies have investigated cemented prostheses. For example, Verdonschot and Huiskes [41] employed physical and numerical models to assess the mechanical effects of stem finish. They found that increasing the surface roughness of a tapered stem ( $R_a$ ,  $\sim 10\ \mu\text{m}$ ) did not necessarily reduce cement damage when compared to a polished stem. In a similar study, Lennon et al. [23] modeled hip prostheses with different interfacial bonding conditions. Their results indicated that a polished stem with an unbonded interface tended to induce more damage to the cement than a matt stem with a bonded interface. Similarly, Jeffers et al. [42] found that a physical prosthetic construction with a polished stem (mean  $R_a = 0.1\ \mu\text{m}$ ) induced more cement fractures, but no substantial fractures were observed in the cement mantle surrounding the grit-blasted stem (mean  $R_a = 2.2\ \mu\text{m}$ ).

### 5.2. Effects of Interface Conditions of Stress

Early studies based on numerical approaches also reported the maximum cement stress in the proximal or distal regions in response to stress within a range of 5.8–16 MPa [36,39,43,44]. The variety of cement stress patterns was probably because different stem designs and loading conditions were used [36,44]. Stolk et al. [44] reported that load distribution in a cemented artificial hip arthroplasty reconstruction was primarily affected by hip joint force and abductor muscles. Inclusions of the ilio-tibial muscle force and the other muscle forces had relatively small effects on stress state of cemented hip composites. In their study, the peak cement stress predicted for bonded and debonded stems predicted under different loading configurations were approximately 3.5 and 9.0 MPa, respectively. In current study, the loading configuration was duplicated from previous study [36], in which the ilio-tibial muscle forces were also included although they were measured to be smaller than other muscles. Under the same loading conditions, current cemented femoral models predicted that much of cements were stressed within 0–4 MPa, approximately 71%, while the model adopted in study of Lennon and Prendergast predicted that there were 79% of cement to be stressed within 0–3 MPa.

In addition, the bonded condition assumed at the cement–stem interface was another factor influencing the cemented femoral model that demonstrated different mechanical behaviors. Harrigan and Harries [45] reported that the peak cement stress greatly increased from 1.4 to 4.6 MPa when the bonding interface of the analysis model was changed from a fully bonded to debonded state. Similarly, Mann et al. [35] found that the cement stresses generated by model with bonded and debonded interfaces were 2.4 and 4.9 MPa, respectively.

In the studies described above, the cemented prosthetic models used in stress analyses were created by implementation of the frictional interface between the cement and the implant, while the friction coefficient was assumed to vary with surface roughness of the implant. As an empirical rule, a friction coefficient of 0.05–0.4 was assumed for polished stems and 0.5–1.0 for roughened stems [46–48]. This modeling approach adopted by Perez et al. [49] led to the conclusion that roughened stems had a higher risk of cement failure than polished stems. However, these findings were in contrast with the results of a study conducted by Jeffers et al. [42]. The inconsistent conclusions drawn from the smooth or rough stems were ascribed to the fact that the contact stiffness and frictional characteristics introduced by the surface-to-surface contact modeling approach were determined based on the stiffness of the material and the surface morphology of the bonded interfaces, which influenced the contact regions to a different extent under the applied loads [50]. In the surface contact mode, the joint load was only transferred through the node pairs, which were maintained at sticking or slipping contact under compressive stress. Therefore, the contact regions varying under the assumed contact conditions affected the load transferring path across the interface and then yielded different cement stress patterns, as previously reported [35,42,46–50].

Unlike the surface contact mode with interface bonding conditions assumed for a polished or roughened stem in previous studies, in this study, we simulated the cemented interface by using an elastic layer with adequate stiffness. This was performed because joint load can also be delivered locally from the implant to the cement and bone under tensile loading as long as the node pairs on the bonded interfaces remain in the elastic bond state, unless the local bonding was destroyed, causing substantial separation between the pairs. The elastic interfacial characteristics (tensile and shear strengths) were experimentally verified to vary with the surface finish of the stem. In essence, the shearing strength was affected by the frictional effect of surface asperities as well as adhesion between the cement and the metal. These characteristics were also incorporated into the finite element simulation model through the proposed elastic spring layer model. The results obtained by the proposed model obviously showed that stems with different surface roughness induced different stress levels at the cement–stem interfaces.

Survival of artificial hip prosthesis is highly dependent on the integrity of the bonded interfaces between the bone cement and the metallic prosthesis. Accordingly, in this study, the mechanical effect derived from the use of roughened or smooth stems was further assessed by failure analysis of the cemented interface. In addition, deterioration of the interface was usually initiated under tensile loading from the pores or defects that could be formed at the bonding surface during cement polymerization [11,30,51]. Thus, tensile failure of the cemented interface was regarded as the primary mechanism for failure of the femoral prosthesis. As indicated in Section 4.3, for a cemented prosthetic femur with roughened stem, more cement–stem interfaces could be disrupted by higher tensile stress, as compared to the case with polished stems. The obtained results do not reflect the clinically observed long-term failure of cemented prostheses. However, this analysis based on the static failure criteria provided information regarding the short-term mechanical effects of the stem surface finish, which is in accordance with the results of clinical studies [20,52,53]. Based on 4- to 8-year follow-up with radiographic examinations, Valle et al. [20] concluded that a femoral stem with roughened surface ( $R_a \geq 2.0 \mu\text{m}$ ) was more likely to result in mechanical loosening than with satin surface ( $R_a = 0.5 \mu\text{m}$ ). Collis and Mohler [52] monitored the clinical outcomes of total hip replacements with grit-blasted ( $R_a = 2.1 \mu\text{m}$ ) and polished ( $R_a = 0.1 \mu\text{m}$ ) components during short-term follow-up after surgery and found that the grit-blasted components had a lower survival rate (91%) than polished components

(100%). They also found that the femoral components in this examination had the same geometry and were implanted using modern cementing techniques under the same surgical procedures, but with different surface finishes (polished and roughened surfaces). These findings describing the effects of stem surface finish on the postoperative performance of the cemented hip prostheses are similar to the results obtained in this study.

### 5.3. Effects of Stem Surface Finish on Subsidence

On the other hand, migration of the femoral component stem within the medullary canal has been used as evidence of the early failure of artificial hip replacement [54]. The subsidence of the femoral stem is recognized as being related to stem shape design and surface finish [55]. However, different surface finishes of stems can have different mechanical effects on the cement at the cement–bone interface, thus resulting in the progress of subsidence in different post implantation period [56]. Ebramzadeh et al. [55] and Choi et al. [57], respectively, employed physical cemented composite constructions to assess the effects of stem design in terms of geometry and surface finish on migration of the femoral component under cyclic joint loads. Although the migrations were measured at different ranges, their results indicated that polished stems showed a greater migration rate than roughened stems of identical shape and size. It is obvious that the findings regarding stem migration in the cement mantle are also in agreement with the finite element predictions of the present study. Considered the bonding ability to resist migration of the cement–stem interface, the stem with the roughened surface was superior to the smooth stem. Nevertheless, the results of the present study showed that a roughened stem was associated with a higher probability of failure of the cement mantles and at the cement–stem interfaces, which would increase the subsidence of subsequent gait loadings [4,23] and initial loss of fixation of the implant [45]. Norman et al. [58] also reported that stem–cement interface friction was a factor affecting the stem subsidence; however, as compared with rough stems, the polished stems have a greater potential to stabilize the debonded stem due to taper locking effect from the increasing cement–stem interface.

Consequently, the analysis results clearly suggest that a femoral stem with a roughened surface is unfavorable for stabilizing the mechanical performance of the hip prosthesis when compared to a smooth stem. By means of the experimental and finite element approaches, this study has demonstrated the difference in the mechanical performances of cemented hip implants with different surface finish. As a quantification analysis, the cemented stem with polished surface ( $R_a = 0.15 \mu\text{m}$ ) and blasting surface ( $R_a = 5.56 \mu\text{m}$ ) were found to show different failure rates at the bonding interface and cement mantles, respectively.

### 5.4. Limitations and Implications

For further application in evaluating the performance of cemented prosthetic implant with various surface textures, there are some limitations to the proposed method. As presented in the analysis model, the cement–stem interfaces around stem were assumed to have homogenous characteristics. This assumption did not consider the variation of locally substantial bonding between the bone cement and the metallic stem which can be processed to uneven or different surface morphology by blasting method with multiply grit sizes, causing the strength to scatter in a wider range [13,14]. In addition, the interface characteristics, which were the vital factors in modeling the cemented prosthetic stem model, were experimentally measured as the fracture force over the bonding area of interface specimens, also termed apparent strengths. As indicated in published literature [7,11,12,30], during the preparation of the interface specimens, the use of cements of different viscosity and metal specimens with different surface treatment might produce porosity to some extent at interfaces, thus contributing to the high variation of the interface characteristics. Consequently, as suggested in [14], experiments with smaller scale interface specimens may be more appropriate to describe the micro-mechanical characteristic of the interface as well as the local failure behavior [59].

Another shortcoming of the study is that the fatigue failure behavior was not concerned as we focused only on static strength tests, and the failure of cemented interfaces and fracture of cement mantles were assessed under physiological gait loading of static mode. Therefore, the analysis results can only reflect the influence of the surface roughness on short-term fixation function of a cemented implant. Clinically, the failure of cemented hip prostheses is well known as a long-term failure scenario, which was characterized as the fatigue fracture propagation of the cement mantles and the progressive debonding of the cemented interface with the increasing gait loadings [4,5]. In vitro studies on commercial cemented synthetic femurs have observed the formation of micro-cracking initiated at the stem–cement interface and then propagating towards the cortical bone of the femur under cyclic loadings [4,60]. To examine such fatigue failure behavior, the fatigue properties of the cemented interface associated with the fatigue failure model should be taken into consideration in finite element modeling of the cemented model. Essentially, the fatigue debonding behavior of the stem–cement interface could be modeled by means of the Paris law model integrated with the experimentally measured crack propagation rate under cyclic loadings [61,62]. It could also be predicted through the use of linear elastic fracture mechanics integrated with the measurement of the fracture property [51,62].

To gain deeper insight into fixation failure of the cemented interface, the mutual influence of cement–stem and cement–bone interfaces should be investigated. Our previous study [32,62] demonstrated the effectiveness of the interface spring element for modeling the debonding behavior of the cement–bone interface, in which the interfacial fracture toughness was quantified by implementing the experimental measured interfacial static strengths into the finite element model of bimaterial specimen. Our future studies will extend the experimental and computational model proposed in this study to investigate the long-term mechanical failure of cemented hip prostheses based on the interaction of two bimaterial interfaces.

## 6. Conclusions

In this study, we illustrated the effect of stem surface finish on the mechanical behavior of cemented prostheses through mechanical strength tests and finite element modeling. Experimental measurements showed that, when compared to the roughened surface, the polished metal had superior bonding ability with bone cement under tensile loading. In contrast, the roughened metal generated higher interface strengths when resisting shearing loading. Further examination of the effect of stem surface finish was conducted based on failure probability analysis combined with the stressed volume concept. The finite element models predicted that the polished stem induced a lower probability of failure of the cement mantle and higher integrity of the cement–stem interface than the roughened stem. These findings are qualitatively consistent with those of comparative studies of the clinical outcomes of cemented femoral components with various surface textures. Finally, the finite element analysis model presented in this study demonstrated that modeling of the bonded interface associated with implementation of the experimentally measured properties is important in investigations of the mechanical behavior of a cemented hip prosthesis.

**Author Contributions:** All authors made contributions to this work. J.-P.H. contributed to the organization of the research work as well as the finite element modeling and manuscript preparation. Y.-W.B. and C.-Q.H. conducted the experimental work on the mechanical tests and data analysis. T.-E.L. conducted data processing and numerical simulations.

**Funding:** This research received no external funding.

**Conflicts of Interest:** The author(s) declared no potential conflicts of interest with respect to the research, authorship, and/or publication of this article.

## References

1. Harris, W.H. The first 32 years of total hip arthroplasty: one surgeon's perspective. *Clin. Orthop. Relat. Res.* **1992**, *274*, 6–11. [[CrossRef](#)]

2. Mohler, C.G.; Callaghan, J.J.; Collis, D.K.; Johnston, R.C. Early loosening of the femoral component at the cement-prosthesis: interface after total hip replacement. *J. Bone Jt. Surg.* **1995**, *77*, 1315–1322. [[CrossRef](#)] [[PubMed](#)]
3. Yang, D.T.; Zhang, D.; Arola, D.D. Fatigue of the bone/cement interface and loosening of total joint replacements. *Int. J. Fatigue* **2010**, *2*, 1639–1649. [[CrossRef](#)]
4. Verdonschot, N.; Huiskes, R. Cement debonding process of total hip arthroplasty stems. *Clin. Orthop. Relat. Res.* **1997**, *336*, 297–307. [[CrossRef](#)] [[PubMed](#)]
5. Jasty, M.; Maloney, W.J.; Bragdon, C.R.; O'Connor, D.O.; Haire, T.; Harris, W.H. The initiation of failure in cemented femoral components of hip arthroplasties. *J. Bone Jt. Surg.* **1991**, *73*, 551–558. [[CrossRef](#)]
6. Chen, Q.Z.; Wong, C.T.; Lu, W.W.; Chung, K.M.C.; Leong, Y.C.Y.; Luk, K.D.K. Strengthening mechanisms of bone bonding to crystalline hydroxyapatite in vivo. *Biomaterials* **2004**, *25*, 4243–4254. [[CrossRef](#)] [[PubMed](#)]
7. Chen, C.Q.; Scott, W.; Barker, T.M. Effect of metal surface topography on mechanical bonding at simulated total hip stem–cement interfaces. *J. Biomed. Mater. Res.* **1999**, *48*, 440–446. [[CrossRef](#)]
8. Sporer, S.M.; Callaghan, J.J.; Olejniczak, J.P.; Goetz, D.D.; Johnston, R.C. The effects of surface roughness and polymethylmethacrylate precoating on the radiographic and clinical results of the Iowa hip prosthesis. A study of patients less than fifty years old. *J. Bone Jt. Surg.* **1999**, *81*, 481–492. [[CrossRef](#)]
9. Davies, J.P.; Harris, W.H. Tensile bonding strength of the cement-prosthesis interface. *Orthopedics* **1994**, *17*, 171–183.
10. Pittman, G.T.; Peters, C.L.; Hines, J.L.; Bachus, K.N. Mechanical bond strength of the cement-tibial component interface in total knee arthroplasty. *J. Arthroplasty* **2006**, *21*, 883–888. [[CrossRef](#)]
11. Zhang, H.; Brown, L.; Blunt, L. Static shear strength between polished stem and seven commercial acrylic bone cements. *J. Mater. Sci. Mater. Med.* **2008**, *19*, 591–599. [[CrossRef](#)] [[PubMed](#)]
12. Wang, J.S.; Taylor, M.; Flivik, G.; Lidgren, L. Factors affecting the static shear strength of the prosthetic stem-bone cement interface. *J. Mater. Sci. Mater. Med.* **2003**, *14*, 55–61. [[CrossRef](#)] [[PubMed](#)]
13. Zhang, H.; Brown, L.T.; Blunt, L.A.; Barrans, S.M. Influence of femoral stem surface finish on the apparent static shear strength at the stem–cement interface. *J. Mech. Behav. Biomed. Mater.* **2008**, *1*, 96–104. [[CrossRef](#)] [[PubMed](#)]
14. Zelle, J.; Janssen, D.; Peeters, S.; Brouwer, C.; Verdonschot, N. Mixed-mode failure strength of implant–cement interface specimens with varying surface roughness. *J. Biomech.* **2011**, *44*, 780–783. [[CrossRef](#)]
15. Meneghini, R.M.; Feinberg, J.R.; Capello, W.N. Primary hybrid total hip arthroplasty with a roughened femoral stem: Integrity of the stem–cement interface. *J. Arthroplasty* **2003**, *18*, 299–307. [[CrossRef](#)]
16. Vail, T.P.; Goetz, D.; Tanzer, M.; Fisher, D.A.; Mohler, C.G.; Callaghan, J.J. A prospective randomized trial of cemented femoral components with polished versus grit-blasted surface finish and identical stem geometry. *J. Arthroplasty* **2003**, *18*, 95–102. [[CrossRef](#)]
17. Lachiewicz, P.F.; Kelley, S.S.; Soileau, E.S. Survival of polished compared with precoated roughened cemented femoral components. A prospective, randomized study. *J. Bone Jt. Surg.* **2008**, *90*, 1457–1463. [[CrossRef](#)] [[PubMed](#)]
18. Gardiner, R.C.; Hozack, W.J. Failure of the cement–bone interface. A consequence of strengthening the cement-prosthesis interface? *J. Bone Jt. Surg.* **1994**, *76*, 49–52. [[CrossRef](#)]
19. Howie, D.W.; Middleton, R.G.; Costi, K. Loosening of matt and polished cemented femoral stems. *J. Bone Jt. Surg.* **1998**, *80*, 573–576. [[CrossRef](#)]
20. Valle, A.G.; Zoppi, A.; Peterson, M.G.E.; Salvati, E.A. A rough surface finish adversely affect the survivorship of a cemented femoral stem. *Clin. Orthop. Relat. Res.* **2005**, *436*, 158–163. [[CrossRef](#)]
21. Costi, K.; Solomon, L.B.; McGee, M.A.; Rickman, M.S.; Howie, D.W. Advantages in using cemented polished tapered stems when performing total hip arthroplasty in very young patients. *J. Arthroplasty* **2017**, *32*, 1227–1233. [[CrossRef](#)] [[PubMed](#)]
22. Hoskins, W.; van Bavel, D.; Lorimer, M.; de Steiger, R.N. Polished cemented femoral stems have a lower rate of revision than matt finished cemented stems in total hip arthroplasty: an analysis of 96,315 cemented femoral stems. *J. Arthroplasty* **2018**, *33*, 1472–1476. [[CrossRef](#)] [[PubMed](#)]
23. Howell, J.R.; Blunt, L.A.; Doyle, C.; Hooper, R.M.; Lee, A.J.C.; Ling, R.S.M. In vivo surface wear mechanisms of femoral components of cemented total hip arthroplasties: the influence of wear mechanism on clinical outcome. *J. Arthroplasty* **2004**, *19*, 88–101. [[CrossRef](#)]

24. Bryant, M.; Farrar, R.; Freeman, R.; Brummitt, K.; Neville, A. The role of surface pre-treatment on the microstructure, corrosion and fretting corrosion of cemented femoral stems. *Biotribology*. **2016**, *5*, 1–15. [[CrossRef](#)]
25. Shearwood-Porter, N.; Browne, M.; Milton, J.A.; Cooper, M.J.; Palmer, M.R.; Latham, J.M.; Wood, R.J.K.; Cook, R.B. Damage mechanisms at the cement–implant interface of polished cemented femoral stems. *J. Biomed. Mater. Res. Part B Appl. Biomater.* **2017**, *105*, 2027–2033. [[CrossRef](#)] [[PubMed](#)]
26. Keller, J.C.; Lautenschlager, E.P.; Marshall Jr, G.W.; Meyer Jr, P.R. Factors affecting surgical alloy/bone cement interface adhesion. *J. Biomed. Mater. Res.* **1980**, *14*, 639–651. [[CrossRef](#)] [[PubMed](#)]
27. Mann, K.A.; Ayers, D.C.; Werner, F.W.; Nicoletta, R.J.; Fortino, M.D. Tensile strength of the cement–bone interface depends on the amount of bone interdigitated with PMMA cement. *J. Biomech.* **1997**, *30*, 339–346. [[CrossRef](#)]
28. Zhang, L.; Ge, S.; Liu, H.; Wang, Q.; Wang, L.; Xian, C.J. Contact damage failure analyses of fretting wear behavior of the metal stem titanium alloy–bone cement interface. *J. Mech. Behav. Biomed. Mater.* **2015**, *51*, 132–146. [[CrossRef](#)]
29. Race, A.; Miller, M.A.; Ayers, D.C.; Cleary, R.J.; Mann, K.A. The influence of surface roughness on stem–cement gaps. *J. Bone Jt. Surg.* **2002**, *84*, 1199–1204. [[CrossRef](#)]
30. Iesaka, K.; Jaffe, W.L.; Kummer, F.J. Integrity of the stem–cement interface in THA: Effects of stem surface finish and cement porosity. *J. Biomed. Mater. Res.* **2008**, *87*, 77–82. [[CrossRef](#)]
31. Chandra, N.; Ghonem, H. Interfacial mechanics of push-out tests: theory and experiments. *Compos. Part A Appl. Sci. Manuf.* **2001**, *32*, 575–584. [[CrossRef](#)]
32. Hung, J.P.; Chang, F.C. Computational modeling of debonding behavior at the bone/cement interface with experimental validation. *Mater. Sci. Eng. C* **2010**, *30*, 445–453. [[CrossRef](#)]
33. Ebramzadeh, E.; Sarmiento, A.; McKellop, H.A.; Llinas, A.; Gogan, A. The cement mantle in total hip arthroplasty. Analysis of long-term radiographic results. *J. Bone Jt. Surg.* **1994**, *76*, 77–78. [[CrossRef](#)] [[PubMed](#)]
34. OrthonNorCal. Cemented hip vs cementless hip replacement implants. Available online: <https://www.orthonorcal.com/cemented-hip-vs-cementless-hip-replacement--implants> (accessed on 19 September 2019).
35. Mann, K.A.; Bartel, D.L.; Wright, T.M.; Burstein, A.H. Coulomb frictional interfaces in modeling cemented total hip replacements: a more realistic model. *J. Biomech.* **1995**, *28*, 1067–1078. [[CrossRef](#)]
36. Lennon, A.B.; Prendergast, P.J. Evaluation of cement stresses in finite element analyses of cemented orthopaedic implants. *J. Biomech. Eng.* **2001**, *123*, 623–628. [[CrossRef](#)]
37. Harper, E.J.; Bonfield, W. Tensile characteristics of ten commercial acrylic bone cements. *J. Biomed. Mater. Res.* **2000**, *53*, 605–616. [[CrossRef](#)]
38. Krause, W.; Mathis, R.S. Fatigue properties of acrylic bone cements: Review of the literature. *J. Biomed. Mater. Res.* **1988**, *22* (A1 Suppl), 37–53.
39. Verdonschot, N.; Huiskes, R. Mechanical effects of stem cement interface characteristics in total hip replacement. *Clin. Orthop. Relat. Res.* **1996**, *329*, 326–336. [[CrossRef](#)]
40. Murphy, B.P.; Prendergast, P.J. On the magnitude and variability of the fatigue strength of acrylic bone cement. *Int. J. Fatigue* **2000**, *22*, 855–864. [[CrossRef](#)]
41. Verdonschot, N.; Huiskes, R. Surface roughness of debonded straight-tapered stems in cemented THA reduces subsidence but not cement damage. *Biomaterials* **1998**, *19*, 1773–1779. [[CrossRef](#)]
42. Jeffers, J.R.T.; Browne, M.; Lennon, A.B.; Prendergast, P.J.; Taylor, M. Cement mantle fatigue failure in total hip replacement: experimental and computational testing. *J. Biomech.* **2007**, *40*, 1525–1533. [[CrossRef](#)] [[PubMed](#)]
43. Hung, J.P.; Wu, J.S.S.; Chen, J.H. Effects of interfacial debonding on fatigue damage of cemented hip prosthesis. *J. Chin. Inst. Eng.* **2003**, *26*, 791–801. [[CrossRef](#)]
44. Stolk, J.; Verdonschot, N.; Huiskes, R. Hip-joint and abductor muscle forces adequately represent in vivo loading of a cemented total hip reconstruction. *J. Biomech.* **2001**, *34*, 917–926. [[CrossRef](#)]
45. Harrigan, T.P.; Harris, W.H. Three-dimensional non-linear finite element study of the effect of cement-prosthesis debonding in cemented femoral total hip components. *J. Biomech.* **1991**, *24*, 1047–1058. [[CrossRef](#)]
46. Nuño, N.; Amabili, M.; Groppetti, R.; Rossi, A. Static coefficient of friction between Ti–6Al–4V and PMMA for cemented hip and knee implants. *J. Biomed. Mater. Res.* **2002**, *59*, 191–200.

47. Nuño, N.; Groppetti, R.; Senin, N. Static coefficient of friction between stainless steel and PMMA used in cemented hip and knee implants. *Clin. Biomech.* **2006**, *21*, 956–962. [[CrossRef](#)] [[PubMed](#)]
48. Stolk, J.; Janssen, D.; Huiskes, R.; Verdonschot, N. Finite element-based preclinical testing of cemented total hip implants. *Clin. Orthop. Relat. Res.* **2007**, *456*, 138–147. [[CrossRef](#)] [[PubMed](#)]
49. Pérez, M.A.; Grasa, J.; García-Aznar, J.M.; Bea, J.A.; Doblaré, M. Probabilistic analysis of the influence of the bonding degree of the stem–cement interface in the performance of cemented hip prostheses. *J. Biomech.* **2006**, *39*, 1859–1872. [[CrossRef](#)]
50. Habraken, A.M.; Cescotto, S. Contact between deformable solids: the fully coupled approach. *Math. Comput. Model.* **1998**, *28*, 153–169. [[CrossRef](#)]
51. Mann, K.A.; Bhashyam, S. Mixed-mode fracture toughness of the cobalt-chromium alloy/polymethylmethacrylate cement interface. *J. Orthop. Res.* **1999**, *17*, 321–328. [[CrossRef](#)]
52. Collis, D.K.; Mohler, C.G. Comparison of clinical outcomes in total hip arthroplasty using rough and polished cemented stems with essentially the same geometry. *J. Bone Jt. Surg.* **2002**, *84*, 586–592. [[CrossRef](#)] [[PubMed](#)]
53. Müller, R.T.; Heger, I.; Oldenburg, M. The mechanism of loosening in cemented hip prostheses determined from long-term results. *Arch. Orthop. Trauma Surg.* **1997**, *116*, 41–45.
54. Krismer, M.; Biedermann, R.; Stöckl, B.; Fischer, M.; Bauer, R.; Haid, C. The prediction of failure of the stem in THR by measurement of early migration using EBRA-FCA. *J. Bone Jt. Surg.* **1999**, *81*, 273–280. [[CrossRef](#)]
55. Ebramzadeh, E.; Sangiorgio, S.N.; Longjohn, D.B.; Buhari, C.F.; Dorr, L.D. Initial stability of cemented femoral stems as a function of surface finish, collar, and stem size. *J. Bone Jt. Surg.* **2004**, *86*, 106–115. [[CrossRef](#)] [[PubMed](#)]
56. Kaneuji, A.; Yamada, K.; Hirosaki, K.; Takano, M.; Matsumoto, T. Stem subsidence of polished and rough double-taper stems: in vitro mechanical effects on the cement–bone interface. *Acta Orthop.* **2009**, *80*, 270–276.3. [[CrossRef](#)] [[PubMed](#)]
57. Choi, D.; Park, Y.; Yoon, Y.S.; Masri, B.A. In vitro measurement of interface micromotion and crack in cemented total hip arthroplasty systems with different surface roughness. *Clin. Biomech.* **2010**, *25*, 50–55. [[CrossRef](#)]
58. Norman, T.L.; Thyagarajan, G.; Saligrama, V.C.; Gruen, T.A.; Blaha, J.D. Stem surface roughness alters creep induced subsidence and ‘taper-lock’ in a cemented femoral hip prosthesis. *J. Biomech.* **2013**, *34*, 1325–1333. [[CrossRef](#)]
59. Waanders, D.; Janssen, D.; Mann, K.A.; Verdonschot, N. The behavior of the micro-mechanical cement–bone interface affects the cement failure in total hip replacement. *J. Biomech.* **2011**, *44*, 228–234. [[CrossRef](#)]
60. Ramos, A.; Simoes, J. In vitro fatigue crack analysis of the Lubinus SPII cemented hip stem. *Eng. Fail. Anal.* **2009**, *16*, 1294–1302. [[CrossRef](#)]
61. Damron, L.A.; Kim, D.G.; Mann, K.A. Fatigue debonding of the roughened stem–cement interface: effects of surface roughness and stem heating conditions. *J. Biomed. Mater. Res. B* **2006**, *78*, 181–188. [[CrossRef](#)]
62. Chang, F.C.; Hung, J.P. Investigation of the fracture characteristics of the interfacial bond between bone and cement: experimental and finite element approaches. *J. Mech. Sci. Tech.* **2010**, *24*, 1235–1244. [[CrossRef](#)]

